Published in final edited form as:
Biomaterials. 2011 May ; 32(14): 3575–3583. doi:10.1016/j.biomaterials.2011.01.062.

The Role of Extracellular Matrix Composition in Structure and Function of Bioengineered Skeletal Muscle

Sara Hinds[1], **Weining Bian**[1], **Robert G Dennis**[2], and **Nenad Bursac**[1,*]

[1] Department of Biomedical Engineering, Duke University, Durham, NC 27708, USA

[2] Department of Biomedical Engineering, University of North Carolina at Chapel Hill, Chapel Hill, NC 27514, USA

Abstract

One of the obstacles to the potential clinical utility of bioengineered skeletal muscle is its limited force generation capacity. Since engineered muscle, unlike most native muscle tissue, is composed of relatively short myofibers, we hypothesized that its force production and transmission would be profoundly influenced by cell-matrix interactions. To test this hypothesis, we systematically varied the matrix protein type (collagen I/fibrin/Matrigel) and concentration in engineered, hydrogel-based neonatal rat skeletal muscle bundles and assessed the resulting tissue structure, generation of contractile force, and intracellular Ca^{2+} handling. After two weeks of culture, the muscle bundles consisted of highly aligned and cross-striated myofibers and exhibited standard force-length and force-frequency relationships achieving tetanus at 40 Hz. The use of 2 mg/ml fibrin (control) yielded isometric tetanus amplitude of 1.4±0.3 mN as compared to 0.9±0.4 mN measured in collagen I-based bundles. Higher fibrin and Matrigel concentrations synergistically yielded further increase in active force generation to 2.8±0.5 mN without significantly affecting passive mechanical properties, tetanus-to-twitch ratio, and twitch kinetics. Optimized matrix composition yielded significant cellular hypertrophy (protein/DNA ratio=11.4±4.1 vs. 6.5±1.9 μg/μg in control) and a prolonged Ca^{2+} transient half-width (Ca_{50}=232.8±33.3 vs. 101.7±19.8 ms). The use of growth-factor-reduced Matrigel instead of standard Matrigel did not alter the obtained results suggesting enhanced cell-matrix interactions rather than growth factor supplementation as an underlying cause for the measured increase in contractile force. In summary, biomaterial-based manipulation of cell-matrix interactions represents an important target for improving contractile force generation in engineered skeletal muscle.

Keywords

Skeletal myoblasts; myogenesis; hydrogel; contractile force

[*]**Corresponding author:** Nenad Bursac Associate Professor of Biomedical Engineering Duke University 3000 Science Drive Hudson Hall Room 136 Durham, NC 27708, USA. Tel.: +1 919 660 5510; fax: + 1 919 684 4488. nbursac@duke.edu.

Introduction

Various pathological conditions such as congenital defects, traumatic injuries, surgical ablations, or degenerative myopathies can lead to considerable loss of skeletal muscle tissue [1-2]. Since the capacity of skeletal muscle to self-regenerate is relatively limited, structural and functional repair of large muscle damage often requires exogenous reconstruction. Unfortunately, current reconstructive strategies, including autologous muscle transposition and the injection of suspended satellite cells or myoblasts, yield only modest therapeutic outcomes due to significant donor-site morbidity as well as poor retention, survival, and integration of grafted cells [2-3]. Recently, implantation of engineered skeletal muscle tissues has been proposed as an alternative strategy with the potential for instant structural repair, prolonged implant survival, and accelerated functional recovery [4-5]. For maximized therapeutic benefit, engineered muscle tissues should recapitulate the structure of the native muscle, i.e., contain densely packed, uniformly aligned muscle fibers enveloped with an appropriate and well-organized extracellular matrix (ECM). *In vivo*, the ECM surrounding individual myofibers, called basal lamina, consists mainly of collagen IV, laminin, and heparin sulphate-containing proteoglycans, which, in addition to the collagen I found in the epimysium and perimysium, provide structural integrity and enable tissue mechanotransduction [6-7]. Moreover, cell-ECM interactions contribute to critical cellular processes during normal muscle growth and development including myogenesis and muscle regeneration [6,8].

The influence of skeletal muscle-derived ECM on myoblast growth and differentiation *in vitro* has been recently explored in a 2-dimensional (2D) setting [9-10]. These studies demonstrated that biomimetic muscle ECM substrates substantially increased the expression of myogenic differentiation markers and enhanced myoblast fusion resulting in formation of large multinucleated myotubes. In a 3-dimensional (3D) setting, naturally derived hydrogels (e.g. collagen I, fibrin and Matrigel) have been often employed as a conducive microenvironment for the biomimetic growth and differentiation of skeletal myoblasts because they support: 1) high density and 3D spreading of muscle cells [11] 2) unidirectional cell alignment through the application of geometric constraints [12] and 3) macroscopic tissue contractions. Although these hydrogel-based muscle tissues have been successfully engineered to contain striated and aligned myotubes [12-16], their contractile forces have been limited to several hundred μN [15-20], i.e. one to two orders of magnitude less than those measured in normal adult muscle. The inferior functional properties of engineered muscle have been attributed to inadequate myotube diameter, volume density, and/or level of functional differentiation.

In this study, we hypothesized that the composition of ECM, which surrounds embedded muscle cells in engineered skeletal muscle, is an important determinant of the contractile function. The rationale for this hypothesis is that significantly shorter myotube length in engineered vs. native muscle (sub mm to mm vs. several mm to several cm) will amplify the role that cell-matrix adhesions play in the generation and transmission of force [21-22]. Thus, the engineered muscle tissue will mainly behave as series-fibered muscles (typical of large, nonprimate mammals) where intrafascicular in-series and in-parallel connections to surrounding matrix and among myofibers significantly affect the total force outcome [23-24]. Therefore, given the same cell density and alignment, the contractile function of the engineered muscle is expected to strongly depend on the type, number, and strength of cell-matrix adhesions, which can be varied by changing the composition and/or concentration of surrounding ECM.

To test this hypothesis, we utilized engineered muscle tissues in the form of hydrogel-based muscle bundles. In this well-controlled system with a linear geometry and uniform 3D cell

alignment we explored the impact of ECM on the tissue formation and function by varying protein type and concentration in a hydrogel matrix and measuring the resulting muscle morphology, force production, and intracellular calcium handling.

Materials and Methods

Isolation of neonatal rat skeletal myoblasts (nSKM)

Primary skeletal myoblasts were isolated from neonatal rats as previously described [25]. Briefly, muscle tissue was dissected from the hindlimbs of 2-3 day old Sprague-Dawley rats, trimmed of excess connective tissue, minced, and digested with 1 mg/ml collagenase type II (Worthington, Lakewood, NJ) in Wyles solution (137mM NaCl, 5mM KCl, 21mM HEPES, 0.7mM Na_2HPO_4, 100mM glucose, and 0.1mg/ml BSA) for 2 hrs at 37° C. Cells were then resuspended in growth medium (DMEM (Gibco Carlsbad, CA), 10% fetal bovine serum (Gibco), 50 U/ml penicillin G (Gibco), 50 μg/ml streptomycin (Gibco), and 5 μg/ml gentamicin (Gibco)) preplated for 2 hours at 37° C to enrich the myoblast fraction, and immediately used for the assembly of bioengineered muscle bundles.

Bioengineered muscle bundle assembly and culture

The protocol for preparing engineered muscle bundles was based on a method developed by Rhim et al [14]. Tissue molds were fabricated by longitudinally splitting a 25 mm long section of 4.7 mm diameter silicone tubing (Nalgene, Rochester, NY) and sealing both ends with a small piece of polydimethylsiloxane (PDMS, Dow Corning, Midland, MI). Molds were sterilized with ethanol, submerged in 0.2% (w/v) pluronic F-127 solution for 1 hr to prevent gel adhesion, dried with nitrogen, and placed in a standard 6-well tissue culture dish. Velcro tabs (~4×4 mm^2), which served as gel attachment sites and allowed generation of passive longitudinal tension in the bundles, were sterilized with ethanol and secured at both ends of the mold with stainless steel pins.

The hydrogel formulation used for engineering of muscle bundles was varied by using different: 1) matrix protein types (collagen I (BD Franklin Lakes, NJ) or fibrinogen (Sigma, St. Louis, MO)), 2) fibrinogen concentrations (2 mg/ml, 4 mg/ml or 6 mg/ml) and 3) percents Matrigel (BD) (10%, 20%, or 40% of total gel volume). Additionally, bundles were prepared with the same percent of Reduced Growth Factor Matrigel (BD) and were compared to those made with standard Matrigel. Isolated nSKMs were mixed with cooled fibrinogen- or neutralized (using 0.1 M NaOH) collagen-containing hydrogel solution to yield a final concentration of 15×10^6 cells/ml. Thrombin (Sigma) (0.5 U per mg fibrinogen) was added to initiate the polymerization of fibrin gels. Four hundred μl of thoroughly mixed cell/gel solution was injected into a silicone tissue mold and incubated for 30 min at 37° C until gelation was completed. Polymerized cell/gel bundles were then maintained in growth medium for 5 days, then switched to low serum differentiation medium (DMEM (Gibco), 3% horse serum (Hyclone, Logan, CT), 50 U/ml penicillin G (Gibco), 50 μg/ml streptomycin (Gibco), and 5 μg/ml gentamicin (Gibco)), and cultured until day 14. Both growth and differentiation media were supplemented with 1 mg/ml 6-aminocaproic acid (Sigma) to inhibit fibrin degradation by serum plasmin.

Functional assessment of bioengineered muscle bundles

On day 14 of culture, muscle bundles were removed from the silicone molds, separated from Velcro anchors, transferred into a custom chamber, and immersed in culture medium at 36±1°C. The bundles were pinned to a fixed tissue holder at one end and to a PDMS floating holder connected to the optical force transducer at the other end. A motorized linear actuator (Thorlabs) controlled the position of the force transducer and length of the bundle, which was independently recorded using a CCD camera (Imagesource) mounted on the top of the

chamber. A pair of parallel platinum electrodes served to apply electrical stimuli and elicit isometric muscle contractions.

After 10 min equilibration, the length of muscle bundle (L) was set to a baseline length (L_0) that generated zero passive tension. Every 2 min, the bundle was elongated by 2% L_0, and a 10 ms, 3 V/mm electrical pulse was applied to induce muscle contraction (twitch). The amplitude of the active twitch and passive tension were recorded as a function of the bundle elongation, L/L_0 (Supplemental Fig. 1A). At the bundle length, L_0*, where maximum twitch amplitude (A_t) was generated, the bundle was stimulated every 2 min for 1 sec at increasing frequencies (1 to 50 Hz) until tetanus was reached (Supplemental Fig. 1B). Parameters of single twitch including amplitude (A_t), the time-to-peak twitch (TPT, from onset of electrical stimulus to time of peak twitch), and half relaxation time ($RT_{1/2}$, from time of peak twitch to 50% recovery time), parameters of tetanus including peak tetanus amplitude (A_T) and time to tetanus (from onset of electrical stimulus to time of tetanus peak), as well as the tetanus-to-twitch ratio ($TtR=A_T/A_t$) were calculated from the recorded traces (Supplemental Fig. 1C) using custom made MATLAB program.

Specific passive tension was calculated (in kPa) by dividing the measured passive tension by the bundle cross-sectional area (derived from bundle image assuming circular cross-section). Muscle bundle stiffness was calculated as the linear slope of the specific passive tension curve for both low (1.02-1.06) and high ($L/L_0* \pm 0.02$) elongations (Supplemental Fig. 1A).

Measurement of intracellular calcium transients

The bioengineered muscle bundles were incubated in serum-free medium containing 5μM calcium sensitive dye Rhod-2 (Molecular probes, Eugene, OR) for 1hr at 37°C, followed by 1hr incubation in dye-free medium. The stained bundles were then transferred into a custom chamber mounted on an inverted fluorescence microscope (Nikon TE2000) and perfused with warm (36°±1°) Tyrode's solution (in mM: 135 NaCl, 5.4 KCl, 1.8 CaCl, 1 MgCl, 0.33 NaHPO, 5 HEPES, 5 glucose). Blebbistatin (5 μM) was added to inhibit contractions and eliminate motion artifacts during recordings [26]. The stained bundles were electrically stimulated (10 ms, 3 V/mm pulses), illuminated by green light (520±25nm) and emitted fluorescence signals (605±30nm) were simultaneously recorded from 504 sites at 2.4 kHz sampling rate and 75 μm resolution using a photodiode array (RedShirt Imaging). The half-width of calcium transient (Ca_{50}) was measured from 50% upstroke to 50% recovery and averaged over all recording sites within the bundle using a custom Matlab software.

Histology

Muscle bundles were fixed in 4% paraformaldehyde overnight at 4°C, rinsed with Dulbecco's phosphate-buffered solution (DPBS, Gibco), dehydrated in ethanol, and embedded in paraffin. Specimens were longitudinally and transversely cut in 10 μm sections and stained with hematoxylin and eosin (H&E). Image J software (NIH, Bethesda, MD) was used to measure the thickness of the dense outer muscle tissue layer containing longitudinally oriented myotubes as well as the average myotube diameter. These thickness measurements served to determine the effective cross-sectional area of the muscle tissue in the bundle, which in turn were used to calculate amplitude of active specific force (in kPa).

Immunostaining

Immunostaining was performed as previously described [12]. Briefly, muscle bundles were fixed in 4% paraformaldehyde (PFA) overnight at 4°C, rinsed with DPBS, permeabilized with 0.5% Triton-X in DPBS for 4 hours at 37°, and blocked with 20% chicken serum/1% bovine serum albumin for 4 hours at 37°C. The bundles were exposed to primary antibodies (sarcomeric α-actinin, Sigma; vimentin, Sigma; integrin α7, Santa Cruz Biotechnology)

overnight at 4°C, followed by secondary antibodies (Alexa 488 and Alexa 594, Molecular Probes) and/or FITC-conjugated phalloidin with nuclear dye (DAPI or propidium iodide, Invitrogen) for 1 hour at room temperature. Images were acquired using a Zeiss confocal microscope (LSM510, Carl Zeiss MicroImaging Inc., Thornwood, NY).

Cellular Protein/DNA Quantification

The muscle bundles were cut in two halves and their wet weights were measured. Each half of the bundle was incubated in DPBS with 10 μg/ml bovine plasmin (Innovative Research, Novi, MI) and 0.5 mg/ml collagenase type II for 2-4 hours at 37°C until matrix was completely dissolved. The total cellular protein content was measured in one bundle half using a BCA™ Protein Assay Kit (Thermo Fisher Scientific, Rockford, IL). The other bundle half was used for the measurement of DNA content. The genomic DNA was isolated from the muscle bundles using a DNeasy tissue kit (Qiagen) and the DNA concentration was measured with a spectrophotometer (NanoDrop 2000, NanoDrop products, Wilmington, DE). The protein/DNA ratio was calculated and normalized for the measured wet-weight ratio.

Statistics

Data are presented as mean ± SE. The difference among multiple groups was analyzed using a repeated measure one-way ANOVA followed by post-hoc Tukey's multiple-comparison test. The differences between two groups were analyzed using a paired value student's t-test. Data were considered statistically significant when $p < 0.05$.

Results

To explore the impact of hydrogel matrix composition on engineered skeletal muscle structure and function, we systematically assessed six types of muscle bundles made of: 1) 1.4 mg/ml collagen I with 10 % Matrigel, 2) 2 mg/ml fibrinogen with 10% Matrigel, 4 mg/ml fibrinogen with 3) 10% Matrigel, 4) 20% Matrigel, or 5) 40% Matrigel, and 6) 6 mg/ml fibrinogen with 10% Matrigel. Significant cell-mediated gel compaction was observed in all muscle bundles starting in first 3 days of culture. After 2 weeks, the bundles (Fig. 1A) have undergone different degrees of compaction depending on both the type and concentration of matrix proteins. Starting from a diameter of 4.7 mm set by the silicon tissue mold, average bundle diameter after 2 weeks ranged from 1.1 ± 0.08 to 2.7 ± 0.18 mm (Fig. 1B). Collagen I-based muscle bundles had the highest degree of compaction (76.6 ± 1.6 %) and, consistent with our previous study [12], exhibited significant rate of rupture (66% in first 5-7 days of culture), while fibrin-based bundles remained intact even when cultured for 5 weeks (not shown). The use of higher fibrinogen and Matrigel concentrations independently and additively reduced the final degree of bundle compaction (Fig. 1B).

As revealed by H&E staining, the muscle bundles after two weeks of culture consisted of an outer region with densely packed cells and a relatively acellular central core (Fig. 2A1-3). For all matrix compositions tested, the outermost cell layer of the dense outer region contained randomly oriented, vimentin-positive fibroblasts. Underneath this cell layer were several layers of longitudinally oriented, multinucleated, and ubiquitously cross-striated myotubes (Fig 2.B&C) that spanned an average depth of 34.7 ± 2.5 μm (similar for different matrix compositions). The myotubes stained positive for laminin-specific α7 integrins [27] (Fig 2.D white arrows) with comparable staining among different groups. As assessed from sarcormeric α-actinin stainings, at two weeks of culture, the percent of the cross-striated myotubes was similar (> 95%) for all hydrogel formulations (not shown).

The engineered muscle bundles began spontaneously contracting 1-2 days after switching to low serum differentiation media (culture day 6-7). Throughout the rest of culture, spontaneous contractions remained spatially uncoordinated and ranged in frequency from 1-3 Hz. After two weeks, electrically stimulated muscle bundles (Supplemental movie 1) displayed biphasic force-length and positive force-frequency relationships, characteristic of native skeletal muscle (Supplemental Fig. 1A & B) [28]. The collagen I-based muscle bundles exhibited the lowest isometric force of contraction with the mean peak twitch (A_t) and tetanus (A_T) amplitudes of 0.59 ± 0.28 mN and 0.88 ± 0.42 mN (Fig. 3A,B), respectively, and the lowest mean tetanus-to-twitch ratio (TtR) of 1.47 ± 0.04. In fibrin-based bundles with 10% Matrigel concentration, the increase of fibrinogen concentration from 2 mg/ml to 6 mg/ml yielded an A_t increase from 0.82 ± 0.20 mN to 1.03 ± 0.24 mN and an A_T increase from 1.40 ± 0.28 mN to 1.89 ± 0.24 mN, respectively (Fig. 3A,B). The bundles containing 6 mg/ml fibrin exhibited the highest TtR of 2.11 ± 0.25. For a constant fibrinogen concentration of 4 mg/ml, increasing the volume percent of Matrigel from 10% to 40% yielded an independent increase in A_t and A_T. Specifically, the muscle bundles containing 40% Matrigel produced the largest isometric forces of contraction among all 6 groups, with an A_t of 1.68 ± 0.32 mN and A_T of 2.84 ± 0.50 mN (Fig. 3A,B). Overall, fibrin-based bundles generated contractile forces up to ~3 fold higher than collagen I-based bundles suggesting a significant impact of cell-matrix interactions on active force generation in engineered muscle tissues. In addition, the generated contractile forces scaled with bundle diameter and, when normalized by the average cross-sectional area of the active muscle layer, the specific forces were found to be comparable among different groups (overall average specific A_t = 5.5 ± 0.6 and A_T = 9.4 ± 0.7 KPa, Supplementary Fig. 2).

We further explored the effect of matrix composition on bundle contraction kinetics by measuring time to peak twitch (TPT), half relaxation time (½RT), and time to tetanus (Fig. 4). The twitch kinetics did not significantly differ between bundles with the varying matrix compositions and averaged for all 6 groups to TPT=58.5 ± 1.6 ms and ½RT=68.2 ± 4.7 ms (Fig. 4). In contrast, the tetanus kinetics were significantly affected by higher concentrations of fibrinogen and Matrigel, which yielded an increase in time to tetanus from 121.3 ± 12 ms for bundles containing 2 mg/ml fibrin and 10% Matrigel to 246.8 ± 15 ms for those containing 4 mg/ml and 40% Matrigel (Fig. 4).

In addition to studying active force generation in muscle bundles, we also assessed their passive mechanical properties (Fig. 5A) by measuring changes in steady-state specific passive tension (tissue stress) as a function of relative bundle elongation (strain). At each elongation, the collagen I-based muscle bundle group exhibited the highest passive tension (Fig. 5A) and stiffness (local slope of the stress-elongation curve) compared to other groups (as shown for low and high elongation, L/L_0, in Fig. 5B). All fibrin-based bundles had comparable stiffness at low L/L_0 while increasing both fibrin concentration and percent Matrigel yielded a significantly decreased stiffness at high L/L_0 (Fig. 5B). In general, muscle bundles with higher stiffness at high L/L_0 generated smaller peak twitch (not shown) and tetanus (Fig. 5C) forces.

In order to further understand how changes in hydrogel composition affect generated contractile force, we compared different muscle bundles with respect to their cell numbers (total DNA content), total cellular protein expression, cell size index (protein/DNA), and average myotube diameter. Specifically, three fibrin-based hydrogel formulations with distinct contents of fibrin and Matrigel were studied (Fig. 6). The total cell number (DNA content) in the muscle bundles was found to be comparable among different hydrogel formulations (Fig. 6A). Simultaneously, the average cellular protein content in the 4 mg/ml fibrinogen + 40% matrigel group (Fig. 6B) was increased 2.54-fold relative to other two groups, without reaching statistical significance (p=0.16). Importantly, the cell size index

(protein/DNA) and average myotube diameter increased significantly for increasing concentrations of fibrin and Matrigel (Fig. 6C,D). The bundles that generated the highest force of contraction (4 mg/ml fibrinogen + 40% Matrigel group) exhibited the largest myotube diameter (14.0 ± 0.5 μm).

We also explored if extracellular matrix composition affected calcium handling of myotubes by recording intracellular calcium transients at different stimulation rates (Fig 7.A). As the stimulation rate was increased to 40 Hz, cytoplasmic calcium concentration in all bundles increased to a constant level (Fig 7.A), which supported the generation of tetanic force. While increase in fibrin concentration had no effect on half-width calcium transient duration (Ca50), the use of 40% Matrigel resulted in a significantly longer Ca50 (232.8 ± 33.3 ms vs. 101 ± 11.4 and 122.4 ± 12.5) (Fig. 7B,C).

Finally, to test if the higher contractile forces in bundles with increased Matrigel concentration were a consequence of growth factors present in Matrigel [29], we compared functional properties of bundles made with standard vs. reduced growth factor (RGF) Matrigel formulation (Fig. 8). We found that the amplitudes and kinetics of contractile force in these two groups were comparable, suggesting that the changes in bundle structure and function induced by varying hydrogel formulations could be attributed to differences in cell-matrix interactions.

Discussion

In this study, we assessed the influence of ECM composition on the structure and function of hydrogel-based engineered neonatal rat skeletal muscle bundles. The most important novel findings of this study are as follows: 1) cell number, alignment, incidence of cross-striations, and rate of spontaneous contractions in engineered muscle bundles were not influenced by the hydrogel matrix composition, 2) the use of fibrin- vs collagen I-based hydrogels resulted in muscle bundles with superior mechanical integrity and force generation capacity, 3) increased hydrogel concentration of fibrin and Matrigel synergistically augmented force generation capacity without affecting the passive mechanical properties of the muscle bundles, and 4) increase in contractile force generation was associated with myofiber hypertrophy and prolongation of intracellular Ca^{2+} transients. The optimal matrix composition (4 mg/ml fibrin with 40% Matrigel) yielded contractile forces (2.84 ± 0.5 mN) that to our knowledge are at least 2-3-fold higher than the maximum force values previously reported for engineered muscle tissues [13,16-19,30].

Our studies revealed that differences in initial hydrogel composition significantly influenced the final diameter of engineered muscle bundles without affecting the total cell number (Fig. 1B and 6A). This result could be attributed to differences in the capacity of embedded cells (i.e., mixture of myoblasts and fibroblasts) to bind and compact hydrogel matrices (collagen I, fibrin, Matrigel) and, potentially, to different degradation rates of fibrin when co-polymerized with varying Matrigel concentrations. Regardless of their effect on bundle diameter, all studied matrix compositions provided conditions necessary to support neonatal rat skeletal myoblast survival, spreading, alignment, fusion, and attainment of significant levels of intracellular structural differentiation characterized by a well-organized sarcomere assembly (Fig. 2C).

Similar to previous reports [13,16], all muscle bundles in this study exhibited qualitatively similar biphasic length-tension and monotonically increasing force-frequency relationships characteristic of native muscle, regardless of the ECM composition. On the other hand, there were several novel results from this study regarding ECM-dependent proprieties of engineered muscle such as the superior contractile force generation (Fig. 3) and lower

stiffness (Fig. 5A) for fibrin- vs. collagen I-based muscle bundles. In addition, fibrinogen concentration did not significantly affect force amplitude, contraction kinetics, Ca^{2+} transient duration, or total protein and DNA (Figs. 3,4,6,7). Interestingly, of all the conditions explored in this study, increasing the Matrigel concentration (from 10% to 40%, with 4 mg/ml fibrin) had the highest impact on bundle force production (71.4% and 64.0% increase in A_t and A_T, respectively), myotube size, and Ca^{2+} transient duration (Figs. 3,6,7). Regarding that Matrigel (Supplementary Table 1) contains different growth factors (e.g. IGF-1 that is shown to enhance contractile force in engineered muscle [16-17]), we compared the function of muscle bundles engineered using standard Matrigel vs. reduced growth factor (RGF) Matrigel (that has decreased levels of IGF-1, PDGF and TGF-β and unchanged concentrations of laminin, collagen IV and entacin) and found no significant difference in isometric force amplitude or twitch and tetanus kinetics (Fig. 8). Thus, another novel and important finding of this study was that the use of higher concentration Matrigel improved force generation capacity of engineered muscle bundles, likely by providing more biologically active cell adhesion sites thereby enhancing myotube-matrix interactions.

Based on these results, we propose that the observed effects of matrix composition on engineered muscle function can be attributed to specific integrin receptors that along with dystrophin complex mediate interaction of myotubes with surrounding endomysial matrix and play important roles in muscle development and force transmission *in vivo* [27]. In particular, laminin-binding α7β1, the dominant integrin in skeletal muscle, is highly expressed at myotendinous junctions, intrafascicular fiber terminations, and the non-junctional sarcolemma [24,31]. This ubiquitous membrane distribution of α7 integrin implies the high importance of myotube-laminin interactions for lateral and longitudinal force transmission in short non-spanning muscle fibers [23-24], such as those present in engineered skeletal muscle. Therefore, we postulate that robust binding of myotubes to laminin via α7 integrins (Fig 2.D) is the main mechanism for significantly improved force generation in engineered muscle bundles with higher Matrigel concentration. In support, a recent study showed that intramuscular or systemic injection of a laminin-111 protein in the *mdx* mouse model of Duchenne muscular dystrophy upregulates α7 integrin expression, which in turn alleviates dystrophic symptoms by stabilizing the sarcolemma and preserving muscle integrity [32].

Similar to α7 integrins, αV integrins, capable of binding to fibrin [33], are expressed in developing and mature myotubes [27], which may explain the positive trend in force generation observed for the increasing fibrin concentrations (Fig. 3). In contrast to α7 and αV integrins, collagen I-specific α2 integrins are not expressed in myoblasts or myotubes, which never directly interact with fibrous collagen I in the native endomysium [27]. This lack of specific myotube-collagen I interactions could contribute to lower contractile forces measured in collagen I- vs. fibrin-based muscle bundles. On the other hand, dominant expression of α2 integrins in fibroblasts [34] may be responsible for the largest compaction and passive tension observed in collagen-based muscle bundles. While it is expected that these integrin-mediated effects were mainly governed by the initial composition of hydrogel matrix, other ECM proteins deposited by cells or adsorbed from culture serum may have also contributed to the obtained results.

Along with the improved force transmission, enhanced cell-matrix interactions likely contributed to the myotube hypertrophy observed in our skeletal muscle bundles (Fig. 6D). Though much remains unknown about the cellular mechanisms involved in integrin-mediated “outside-in” signaling, several integrins, including α7 and αV, are shown to play important roles in triggering the events leading to myoblast migration, fusion, and myotube differentiation [8,27,35-37]. Furthermore, load-activated integrin-mediated signaling was proposed as an important regulator of gene expression in hypertrophying skeletal muscle

leading to increased protein synthesis [38]. Based on these studies, a more robust cell-ECM binding in the presence of higher Matrigel or fibrinogen content in our engineered muscle bundles was expected to promote myotube fusion and/or augment the mechanical load (resistance) experienced by spontaneously contracting myotubes. Both of these factors could have led to the observed increase in myotube diameter.

An interesting finding of this study was the significant prolongation of intracellular calcium transients in engineered muscle bundles with increased Matrigel concentration (Fig. 7B,C). Currently, little is known about the potential role that integrin binding to ECM plays in kinetics of intracellular Ca^{2+} cycling in skeletal muscle. In one study, engagement of α7 integrins with laminin has been shown to trigger transient elevations in free intracellular Ca^{2+} through calreticulin mediated Ca^{2+} signaling [39]. Calreticulin, a Ca^{2+} binding protein that associates with cytoplasmic integrin domain, is known to regulate the coupling of IP_3-sensitive Ca^{2+} release from intracellular stores and influx through L-type Ca^{2+} channels, and may thus be one of the mediators of observed Ca^{2+} transient prolongation. Since the actomyosin contraction mechanism is activated by binding of intracellular Ca^{2+} to troponin [28], it is possible that prolonged Ca^{2+} transients may have directly contributed to the observed slowing of tetanus kinetics (Fig. 4). This possibility will be explored in our future studies.

While hydrogel-based engineered muscle tissues typically contain Matrigel [12,14,40-41], it is well recognized that Matrigel will not be used in humans due to its murine origin and potential tumorigenicity. Thus, future clinical translation would require replacement of Matrigel with a defined combination of commercially available ECM proteins and/or reconstituted human-derived basal lamina matrix [42]. Furthermore, although the muscle fibroblasts embedded in a fibrin gel are expected to synthesize and secrete endogenous extracellular matrix proteins (e.g., collagen I, elastin [43-44]), this process is relatively slow. Consequently, the major contributor to initial myogenesis and functional differentiation of engineered muscle will be exogenous hydrogel matrix, which needs to be carefully customized prior to tissue culture. One potential strategy to augment bioactivity of fibrin gels for skeletal muscle tissue engineering would be enzymatic incorporation of bioactive peptides to engage laminin-binding integrins in muscle cells [45]. In addition, due to the rapid degradation of fibrin *in vivo*, the successful clinical application of fibrin-based engineered skeletal muscle would likely require use of potent cross-linking (e.g. genipin [30], transglutaminase [46]) and anti-fibrinolytic (e.g. engineered aprotinin [47]) agents, or a long-term tissue culture to permit replacement of fibrin by cell-secreted ECM.

Conclusions

In support of our initial hypothesis, we have shown that manipulating hydrogel matrix composition (i.e., cell-matrix interactions) has the potential to significantly improve contractile function of engineered muscle tissue, as demonstrated by a 3-fold increase in force amplitude between collagen I-based and optimized fibrin-based bundles. Importantly, varying hydrogel composition had a larger relative effect on contractile force generation of engineered muscle than the previously reported manipulation of cell microRNA expression, electrical stimulation, co-culture with neuronal cells, or growth factor supplementation. Our results therefore imply that in addition to ultrastructural and functional maturation of individual myofibers, biomaterial-based manipulation of cell-matrix interactions represents another important target for improving overall contractile performance of engineered skeletal muscle. Together with methods for successful vascularization (by use of multiple cell types or growth factors) and innervation (by use of neurotrophic and synaptogenic factors) upon implantation, this strategy holds potential for yielding functional skeletal

muscle substitutes capable of restoring the load-bearing function of diseased or injured muscle.

Supplementary Material

Refer to Web version on PubMed Central for supplementary material.

Acknowledgments

We acknowledge Dr. George Truskey, Caroline Rhim and Cindy Cheng for their advice on the muscle bundle preparation protocol. This work was supported by NIH grant AR055226 from National Institute of Arthritis and Musculoskeletal and Skin Disease to N.B.

References

1. Alsberg E, Hill EE, Mooney DJ. Craniofacial tissue engineering. Crit Rev Oral Biol Med 2001;12:64–75. [PubMed: 11349963]
2. Bach AD, Beier JP, Stern-Staeter J, Horch RE. Skeletal muscle tissue engineering. J Cell Mol Med 2004;8:413–22. [PubMed: 15601570]
3. Vilquin JT. Myoblast transplantation: clinical trials and perspectives. Mini-review. Acta Myol 2005;24:119–27. [PubMed: 16550929]
4. Bian W, Bursac N. Tissue engineering of functional skeletal muscle: challenges and recent advances. IEEE Eng Med Biol Mag 2008;27:109–13. [PubMed: 18799400]
5. Liao H, Zhou GQ. Development and progress of engineering of skeletal muscle tissue. Tissue Eng Part B Rev 2009;15:319–31. [PubMed: 19591626]
6. Velleman SG. The role of the extracellular matrix in skeletal muscle development. Poult Sci 1999;78:778–84. [PubMed: 10228976]
7. Kjaer M. Role of extracellular matrix in adaptation of tendon and skeletal muscle to mechanical loading. Physiol Rev 2004;84:649–98. [PubMed: 15044685]
8. Osses N, Brandan E. ECM is required for skeletal muscle differentiation independently of muscle regulatory factor expression. Am J Physiol Cell Physiol 2002;282:C383–94. [PubMed: 11788350]
9. Stern MM, Myers RL, Hammam N, Stern KA, Eberli D, Kritchevsky SB, et al. The influence of extracellular matrix derived from skeletal muscle tissue on the proliferation and differentiation of myogenic progenitor cells ex vivo. Biomaterials 2009;30:2393–9. [PubMed: 19168212]
10. DeQuach JA, Mezzano V, Miglani A, Lange S, Keller GM, Sheikh F, et al. Simple and high yielding method for preparing tissue specific extracellular matrix coatings for cell culture. PloS one 2010;5:e13039. [PubMed: 20885963]
11. Okano T, Satoh S, Oka T, Matsuda T. Tissue engineering of skeletal muscle. Highly dense, highly oriented hybrid muscular tissues biomimicking native tissues. Asaio J 1997;43:M749–53. [PubMed: 9360146]
12. Bian W, Bursac N. Engineered skeletal muscle tissue networks with controllable architecture. Biomaterials 2009;30:1401–12. [PubMed: 19070360]
13. Yan W, George S, Fotadar U, Tyhovych N, Kamer A, Yost MJ, et al. Tissue engineering of skeletal muscle. Tissue Eng 2007;13:2781–90. [PubMed: 17880268]
14. Rhim C, Lowell DA, Reedy MC, Slentz DH, Zhang SJ, Kraus WE, et al. Morphology and ultrastructure of differentiating three-dimensional mammalian skeletal muscle in a collagen gel. Muscle Nerve 2007;36:71–80. [PubMed: 17455272]
15. Yamamoto Y, Ito A, Fujita H, Nagamori E, Kawabe Y, Kamihira M. Functional evaluation of artificial skeletal muscle tissue constructs fabricated by a magnetic force-based tissue engineering technique. Tissue Eng Part A 2011;17:107–14. [PubMed: 20672996]
16. Huang YC, Dennis RG, Larkin L, Baar K. Rapid formation of functional muscle in vitro using fibrin gels. J Appl Physiol 2005;98:706–13. [PubMed: 15475606]

17. Vandenburgh H, Shansky J, Benesch-Lee F, Barbata V, Reid J, Thorrez L, et al. Drug-screening platform based on the contractility of tissue-engineered muscle. Muscle Nerve 2008;37:438–47. [PubMed: 18236465]
18. Lam MT, Huang YC, Birla RK, Takayama S. Microfeature guided skeletal muscle tissue engineering for highly organized 3-dimensional free-standing constructs. Biomaterials 2009;30:1150–5. [PubMed: 19064284]
19. Rhim C, Cheng CS, Kraus WE, Truskey GA. Effect of microRNA modulation on bioartificial muscle function. Tissue Eng Part A 2010;16:3589–97. [PubMed: 20670163]
20. Frueh BR, Gregorevic P, Williams DA, Lynch GS. Specific force of the rat extraocular muscles, levator and superior rectus, measured in situ. Journal of neurophysiology 2001;85:1027–32. [PubMed: 11247972]
21. Monti RJ, Roy RR, Hodgson JA, Edgerton VR. Transmission of forces within mammalian skeletal muscles. J Biomech 1999;32:371–80. [PubMed: 10213027]
22. Patel TJ, Lieber RL. Force transmission in skeletal muscle: from actomyosin to external tendons. Exercise and sport sciences reviews 1997;25:321–63. [PubMed: 9213097]
23. Young M, Paul A, Rodda J, Duxson M, Sheard P. Examination of intrafascicular muscle fiber terminations: implications for tension delivery in series-fibered muscles. Journal of morphology 2000;245:130–45. [PubMed: 10906747]
24. Paul AC, Sheard PW, Kaufman SJ, Duxson MJ. Localization of alpha 7 integrins and dystrophin suggests potential for both lateral and longitudinal transmission of tension in large mammalian muscles. Cell Tissue Res 2002;308:255–65. [PubMed: 12037582]
25. Bian W, Liau B, Badie N, Bursac N. Mesoscopic hydrogel molding to control the 3D geometry of bioartificial muscle tissues. Nature protocols 2009;4:1522–34.
26. Fedorov VV, Lozinsky IT, Sosunov EA, Anyukhovsky EP, Rosen MR, Balke CW, et al. Application of blebbistatin as an excitation-contraction uncoupler for electrophysiologic study of rat and rabbit hearts. Heart Rhythm 2007;4:619–26. [PubMed: 17467631]
27. Mayer U. Integrins: redundant or important players in skeletal muscle? J Biol Chem 2003;278:14587–90. [PubMed: 12556453]
28. King AM, Loiselle DS, Kohl P. Force generation for locomotion of vertebrates: Skeletal muscle overview. Ieee J Oceanic Eng 2004;29:684–91.
29. Vukicevic S, Kleinman HK, Luyten FP, Roberts AB, Roche NS, Reddi AH. Identification of Multiple Active Growth-Factors in Basement-Membrane Matrigel Suggests Caution in Interpretation of Cellular-Activity Related to Extracellular-Matrix Components. Experimental Cell Research 1992;202:1–8. [PubMed: 1511725]
30. Khodabukus A, Baar K. Regulating fibrinolysis to engineer skeletal muscle from the C2C12 cell line. Tissue Eng Part C Methods 2009;15:501–11. [PubMed: 19191517]
31. Mayer U, Saher G, Fassler R, Bornemann A, Echtermeyer F, von der Mark H, et al. Absence of integrin alpha 7 causes a novel form of muscular dystrophy. Nat Genet 1997;17:318–23. [PubMed: 9354797]
32. Rooney JE, Gurpur PB, Burkin DJ. Laminin-111 protein therapy prevents muscle disease in the mdx mouse model for Duchenne muscular dystrophy. Proc Natl Acad Sci U S A 2009;106:7991–6. [PubMed: 19416897]
33. Katagiri Y, Hiroyama T, Akamatsu N, Suzuki H, Yamazaki H, Tanoue K. Involvement of alpha v beta 3 integrin in mediating fibrin gel retraction. J Biol Chem 1995;270:1785–90. [PubMed: 7530248]
34. Klein CE, Dressel D, Steinmayer T, Mauch C, Eckes B, Krieg T, et al. Integrin alpha 2 beta 1 is upregulated in fibroblasts and highly aggressive melanoma cells in three-dimensional collagen lattices and mediates the reorganization of collagen I fibrils. J Cell Biol 1991;115:1427–36. [PubMed: 1955483]
35. Menko AS, Boettiger D. Occupation of the extracellular matrix receptor, integrin, is a control point for myogenic differentiation. Cell 1987;51:51–7. [PubMed: 3115595]
36. Yao CC, Ziober BL, Sutherland AE, Mendrick DL, Kramer RH. Laminins promote the locomotion of skeletal myoblasts via the alpha 7 integrin receptor. J Cell Sci 1996;109(Pt 13):3139–50. [PubMed: 9004048]

37. Wilschut KJ, Haagsman HP, Roelen BA. Extracellular matrix components direct porcine muscle stem cell behavior. Exp Cell Res 2010;316:341–52. [PubMed: 19853598]

38. Carson JA, Wei L. Integrin signaling's potential for mediating gene expression in hypertrophying skeletal muscle. J Appl Physiol 2000;88:337–43. [PubMed: 10642399]

39. Kwon MS, Park CS, Choi K, Ahnn J, Kim JI, Eom SH, et al. Calreticulin couples calcium release and calcium influx in integrin-mediated calcium signaling. Mol Biol Cell 2000;11:1433–43. [PubMed: 10749940]

40. Powell C, Shansky J, Del Tatto M, Vandenburgh HH. Bioartificial muscles in gene therapy. Methods Mol Med 2002;69:219–31. [PubMed: 11987780]

41. Zimmermann WH, Schneiderbanger K, Schubert P, Didie M, Munzel F, Heubach JF, et al. Tissue engineering of a differentiated cardiac muscle construct. Circ Res 2002;90:223–30. [PubMed: 11834716]

42. Siegal GP, Wang MH, Rinehart CA Jr. Kennedy JW, Goodly LJ, Miller Y, et al. Development of a novel human extracellular matrix for quantitation of the invasiveness of human cells. Cancer Lett 1993;69:123–32. [PubMed: 8495401]

43. Clark RA, Nielsen LD, Welch MP, McPherson JM. Collagen matrices attenuate the collagen-synthetic response of cultured fibroblasts to TGF-beta. J Cell Sci 1995;108(Pt 3):1251–61. [PubMed: 7622608]

44. Long JL, Tranquillo RT. Elastic fiber production in cardiovascular tissue-equivalents. Matrix Biol 2003;22:339–50. [PubMed: 12935818]

45. Schense JC, Bloch J, Aebischer P, Hubbell JA. Enzymatic incorporation of bioactive peptides into fibrin matrices enhances neurite extension. Nat Biotechnol 2000;18:415–9. [PubMed: 10748522]

46. Orban JM, Wilson LB, Kofroth JA, El-Kurdi MS, Maul TM, Vorp DA. Crosslinking of collagen gels by transglutaminase. J Biomed Mater Res A 2004;68:756–62. [PubMed: 14986330]

47. Lorentz KM, Kontos S, Frey P, Hubbell JA. Engineered aprotinin for improved stability of fibrin biomaterials. Biomaterials 2011;32:430–8. [PubMed: 20864171]

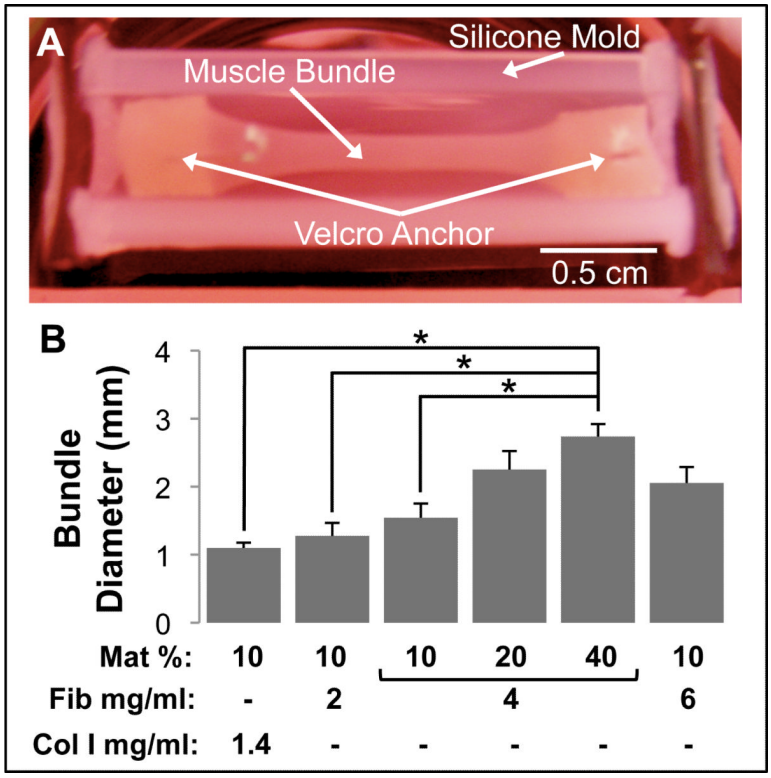

Figure 1.

Morphology of bioengineered skeletal muscle bundles. (A) A representative muscle bundle shown in a silicone tissue mold. The muscle bundle was anchored at each end to pinned Velcro® tabs. (B) Final muscle bundle diameter on culture day 14 for the 6 studied hydrogel formulations. The hydrogel formulations contained different volume percent Matrigel (Mat %), fibrinogen concentration (Fib mg/ml) and collagen I concentration (Col I mg/ml). Bars show n=3 bundles per group. '*', statistically significant between the indicated pairings, $p<0.05$.

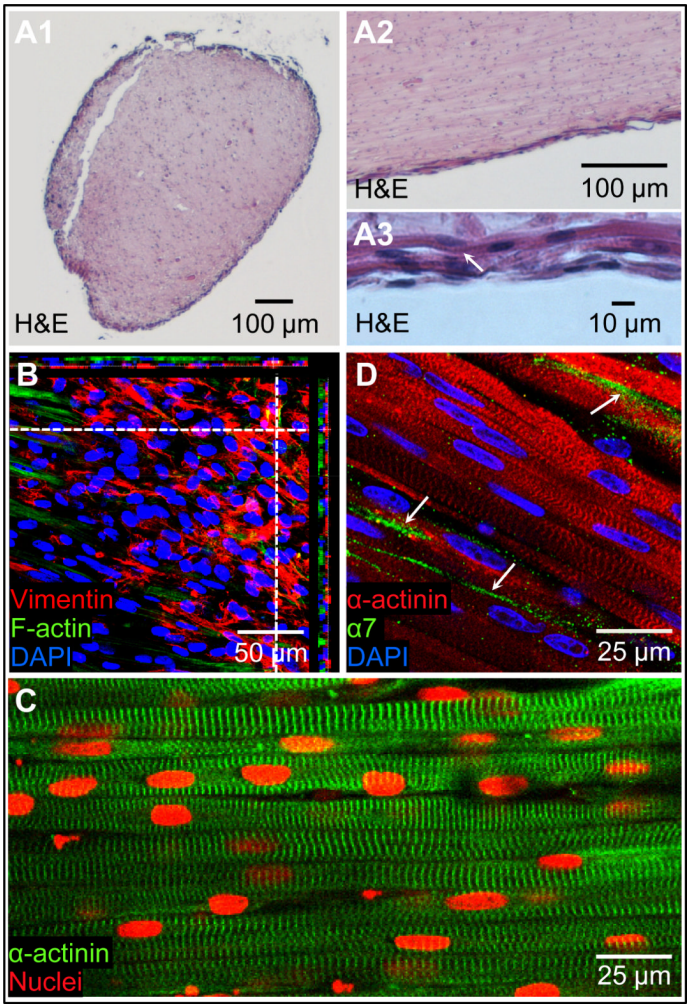

Figure 2.

Structure of bioengineered skeletal muscle bundles. (A1-3) Representative H&E stainings of a day 14 muscle bundle showing densely packed myotubes, located in the outer bundle region (A1), that were longitudinally oriented (A2-3). White arrow in A3 indicates visible cross-striations. (B) Confocal stack image of a day 14 bundle. Top and right frames are front and side views of the stack, respectively. Note that fibroblasts (red) form a single outermost layer on the bundle surface and cover muscle layers underneath (green). (C) A representative confocal section ~20 μm below the bundle surface shows that aligned multinucleated myotubes exhibit ubiquitous cross-striations. (D) Typical immunostaining for α7 integrins (green, white arrows) along myotube membrane. Panels A1-3, B, and D are from muscle bundles with 4 mg/ml fibrinogen and 10% Matrigel, while panel C is from a muscle bundle with 4 mg/ml fibrinogen and 40% Matrigel.

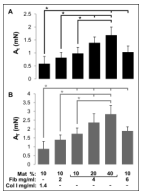

Figure 3.

Contractile force generation in bioengineered skeletal muscle bundles. (A,B) Peak twitch (A_t) and tetanus (A_T) amplitudes for the 6 studied hydrogel formulations. The nomenclature describing hydrogel formulations is the same as shown in figure 1. Bars from left to right are obtained from n=4, 7, 8, 7, 7, and 6 bundles per group. '*', statistically significant between the indicated pairings, $p<0.05$.

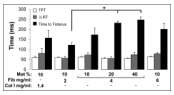

Figure 4.
Kinetics of contractile force generation in bioengineered skeletal muscle bundles. Time to peak twitch (TPT), half-relaxation time (1/2RT), and time-to-tetanus are shown for the 6 studied hydrogel formulations. The nomenclature describing hydrogel formulations and number of bundles per group are the same as shown in figure 3. '*', statistically significant between the indicated pairings, $p<0.05$.

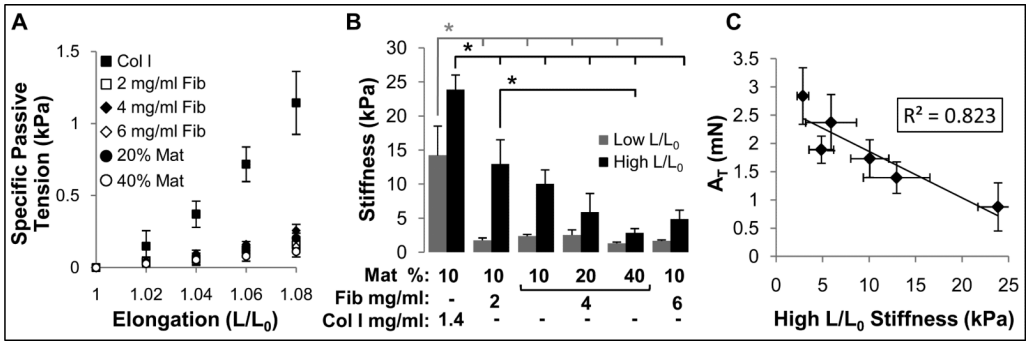

Figure 5.

Passive mechanical properties of bioengineered skeletal muscle bundles. (A) Specific passive tension (stress) as a function of bundle elongation (L/L_0) shown for the 6 studied hydrogel formulations. Note increased stress in collagen I-based vs. fibrin-based bundles. The groups without indicated Mat% contain 10% Matrigel, while those with only indicated % Mat contain 4 mg/ml fibrinogen. (B) Muscle bundle stiffness at high and low L/L_0. The nomenclature describing hydrogel formulations (bundle groups) is the same as shown in figure 1. (C) Correlation between tetanus amplitude (A_T) and bundle stiffness at high elongation in all 6 studied bundle groups. Number of bundles per group is the same as in figure 3. '*', statistically significant between the indicated pairings, $p<0.05$.

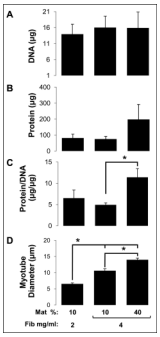

Figure 6.

Indices of cell number and size in fibrin-based skeletal muscle bundles. (A) Total DNA content (index of cell number) in bundles. (B) Total cellular protein content in bundles. (C) Cellular protein/DNA ratio (index of average cell size) in bundles. (D) Average myotube diameter in bundles. The nomenclature describing hydrogel formulations is the same as in figure 1. For A-C, n=4 bundles per group; For D, n=3 bundles per group. '*', statistically significant between the indicated pairings, $p<0.05$.

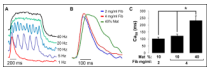

Figure 7.

Intracellular Ca^{2+} transients in fibrin-based skeletal muscle bundles. (A) Representative optically recorded traces of intracellular Ca^{2+} concentration for different stimulation frequencies. Note that increasing pacing frequency yields a sustained elevated level of intracellular Ca^{2+} concentration. (B) Representative single Ca^{2+} transients for 3 studied hydrogel compositions showing differences in the transient duration. (C) Half-width of the Ca^{2+} transient duration (Ca_{50}) in engineered bundles. Bars show n=3 bundles per group. The nomenclatures describing hydrogel compositions are the same as in figure 5. '*', statistically significant between the indicated pairings, $p<0.05$.

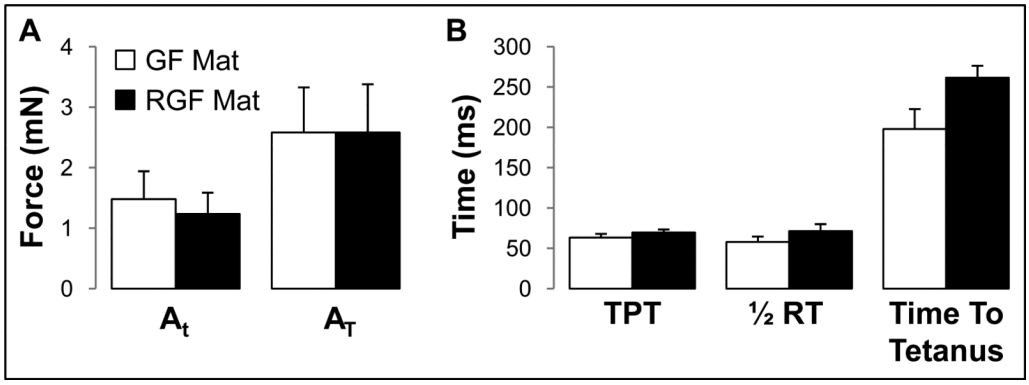

Figure 8.

Comparison of contractile force generation in bioengineered skeletal muscle bundles made using standard vs. reduced growth factor (RGF) Matrigel. (A) Twitch (A_t) and tetanus (A_T) amplitudes. (B) Kinetic parameters of twitch and tetanus, with nomenclature defined in figure 4. Muscle bundles were made with 4 mg/ml Fibrinogen and 40% standard or RGF Matrigel. Bars show n=3 bundles per group.